Int. J. Electrochem. Sci., 6 **(2011)** 4648 - 4666

International Journal of
ELECTROCHEMICAL
SCIENCE
www.electrochemsci.org

Water Transport in Composite Membranes Containing Silica: Temperature and Relative Humidity Effects

C. Guzmán[1], A. Alvarez[1], O.E. Herrera[2], R. Nava[3], J. Ledesma-Garcia[3], Luis A. Godínez[1], L.G. Arriaga[1,], W. Mérida[2,§].*

[1] Centro de Investigación y Desarrollo Tecnológico en Electroquímica S.C., C.P. 76703, Querétaro, México.
[2] Clean Energy Research Centre, University of British Columbia, Vancouver, B.C., Canada, V6T1Z4.
[3] División de Investigación y Posgrado, Facultad de Ingeniería, Universidad Autónoma de Querétaro, C.P. 76010, Querétaro, México.
[*]E-mail: larriaga@cideteq.mx
[§]E-mail: walter.merida@ubc.ca

Received: 7 April 2011 / *Accepted:* 2 September 2011 / *Published:* 1 October 2011

The aim of this work is to show the water flux across composite proton exchange membranes containing silica and SBA-15 fillers. The experiments were carried out using a gated cell in order to control the temperature and relative humidity (80 to 100 ºC, and 10, 50, 100%, respectively). The morphology was studied by scanning electron microscopy (SEM) and EDXS. The EDXS presents the characteristic signals of Nafion and their corresponding signal of Si attributed to the inorganic material and the SEM images showed a homogeneous dispersion of the material on the membrane. Composite membranes showed higher water flux (77 mmol m^{-2} s^{-1}) at simulated high temperature fuel cell conditions than the commercial Nafion membrane (67 mmol m^{-2} s^{-1}). On the fuel cell test, the composite membranes exhibited better performance at 40% RH and 120 °C with a power density of 0.15, 0.14 and 0.12 Wcm^{-2} for composite (SiO_2 and SBA15) and Nafion membranes. These results placed these composite membranes as a very promising material for application in high temperature fuel cells and low relative humidity.

Keywords: Composite membranes, Nafion, SiO_2 membrane, SBA–15 membrane, water flux, low relative humidity, high temperature PEMFC's.

1. INTRODUCTION

Water transport phenomena have a strong impact on the efficiency and power of a proton exchange membrane fuel cell (PEMFC). PEMFC's are typically operated below 100 °C (80 °C and

fully humidified reaction gases). Poor water quantity in the system decreases the proton conductivity and increases the cell resistance and the cell voltage decreases. Unnecessary water amounts in the cathode causes flooding; the water blocks the supply gases in the porous media resulting in mass – transport limitations, increasing the cathode overvoltage, and in considerable power losses in the PEMFC. In order to prevent this effect in the PEMFC's systems is necessary to develop new strategies to maintain an adequate balance in the operation of these systems.

Research efforts are focused on the operation of PEMFC's at high temperatures (above 100 °C). At this condition the water management can be simplified and a single water phase of water need to be considered and the reaction gases can be introduced with lows amounts of water [1-3]. Other advantages of work in environments of high temperature and low relative humidity are (I) the kinetics of the oxygen reduction reaction is enhanced [3, 4]; (II) the CO tolerance are improved [3, 5-8]; (III) The cooling system can be omitted [3]; and (IV) waste heat can be recovered [2, 3, 9] In this context, previous reports indicate that the high temperature (120 ºC) PEMFC performance can improve due to more facile kinetics for the relevant reactions [10].

Nevertheless, Nafion is the most popular membrane for PEMFC's. It has been operated below 80 ºC and high humidity conditions (80–100 %). Under these conditions it can reach its maximum proton conductivity ($\sigma \geq 10^{-2}$ Scm^{-1}) [11-13]. However, when the fuel cell temperature increases, the conductivity decreases dramatically due to membrane dehydration, which can result in low cell performance leading to significant ohmic losses within the cell [14].

Several approaches have been developed in order to improve Nafion properties. One effective procedure consist in the incorporation of inorganic materials as Al_2O_3 [15], SiO_2 [15, 16], ZrO_2 [16, 17] and TiO_2 [17, 18]. These compounds can improve the water retention as well as the mechanical properties of the membrane [11, 14-18]. The inclusion of inorganic oxides confers a new membrane arrangement that inhibits the permeation of the reactant gases [18]. In addition, water molecules are strongly coordinated to the dipoles or ions in the inorganic material, enhancing the membrane hydration [19, 20].

The aim of the present work was to determinate the vapor water flux (J), under steady – state conditions and the PEMFC performance, using inorganic fillers based on silicon dioxide; as a function of the temperature and the relative humidity. The results obtained were compared with a commercial membrane (Nafion 115).

2. EXPERIMENTAL

2.1 Synthesis of the inorganic fillers

Siliceous SBA-15 mesoporous material was synthesized following a method published previously [21-23]. Pluronic P123 (EO20PO70EO20, BASF) dissolved in a solution of water and 4M HCl was used as the structure directing agent. Tetraethyl orthosilicate (TEOS 98%, Aldrich) was used as a silica source and was added to the Pluronic solution at 35°C under stirring for 24 h. Subsequently, the mixture was heated at 80 °C for 24 h. The resulting solid was filtered, washed with excess

deionized DI water and dried at 110 °C for 18 h. Finally, the product was thermally treated at 500 °C for 6 h to remove the organic template. Silica was synthesized via sol-gel method under acidic conditions. TEOS was used as precursor with HNO_3 as catalyst. Alcohol/alkoxide molar ratio was kept under stirring for 20 minutes. Water/acid molar ratio remained under constant stirring for 5 minutes. Finally, both solutions were mixed under stirring for 1h at 40 ° C. This colloidal solution was kept at room temperature until solid formation. The resulting solid was thermally treated using a tubular furnace (Barnstead Thermolyne) at 150°C for 2 h in order to remove residual alcohol and finally obtaining the silicon dioxide [24-30].

2.2 Membrane Preparation

Composite membranes containing 97 wt. % of Nafion (Nafion solution 5 %) and 3 wt. % inorganic fillers were prepared using a combination of recast and heat treatment procedures already described [31]. Subsequent chemical treatments included a 3% H_2O_2 solution followed by a 0.5M H_2SO_4 solution with intermediate boiling steps using DI water [32, 33]. Finally the membranes were stored in DI water for at least 24 h prior to use. Composite membranes were drying at 80 °C during 20 h, before to the water flux experiments.

2.3 Physicochemical characterization of the composite membranes

The synthesized powders (SiO_2 and SBA – 15) were first analyzed by X-ray diffraction measurements were performed on a DMAX 2100 Rigaku diffractometer using CuKα monochromatic radiation in the range of 10° to 90°. The membrane morphology was studied by Scanning Electron Microscopy (SEM) in a JEOL JSM-6060 LV microscope and the surface mapping by energy dispersive X-ray spectroscopy (EDXS).

2.4 Water transport experiments

The different setups used for the Water Transport experiments are illustrated in figure 1 a and b. The experimental cell [34] consists in two chambers separated by $2cm^2$ of the composite membranes. Hot water was circulated through double – walled chambers to control the temperature, on one chamber (dry chamber) was introduced dry helium gas and server as the carrier gas for the permeate water from the other chamber. On the dry chamber were placed fine wire thermocouples (omega®) and two pressure transducers (MSP 340) used to monitoring the temperature and pressure of the system. For the water transport measurements was placed a dew point sensor (Vaisala® HMT 330) previously cross – referenced with an RGA – mass spectrometer showing that the dew point sensor had a smaller maximum error compared to the mass spectrometer (2.7% and 6.7% in the whole temperature testing, respectively) [34]. On the other chamber (wet side), Nitrogen was used to enhance the water vaporization into the wet chamber (figure 1a) and maintaining constant the relative humidity.

In order to change the relative humidity (figure 1b) the nitrogen was introduced using a Green light Power Station (Green light power technologies FCATS – S 800).

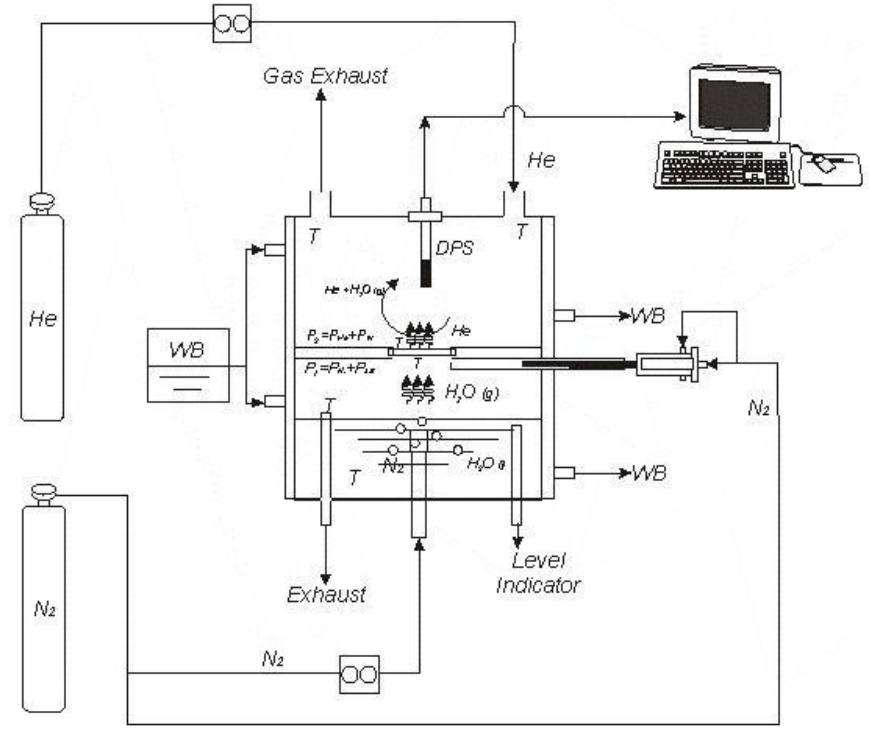

A)

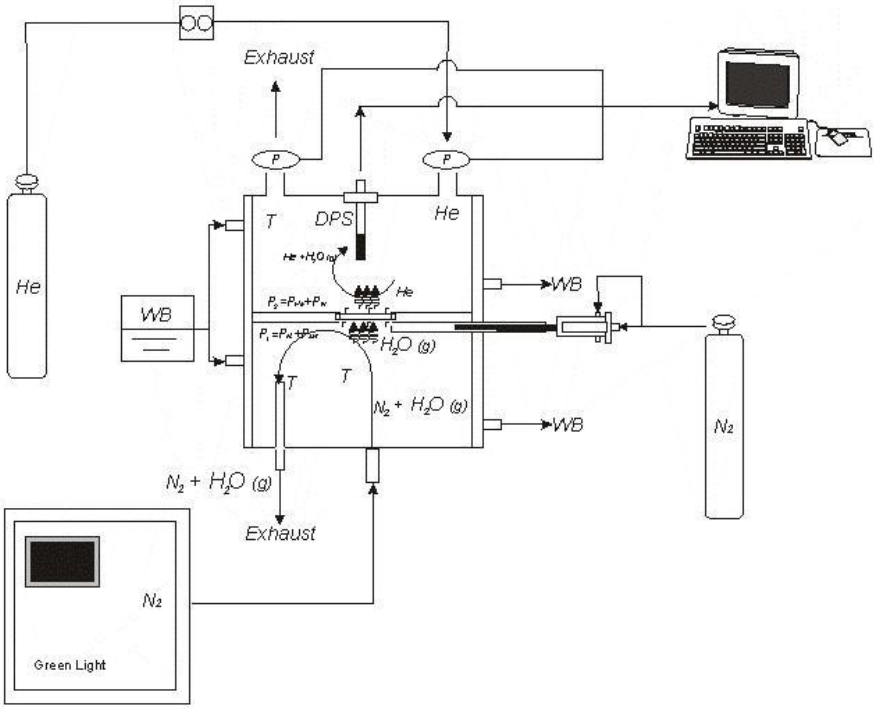

B)

Figure 1. Complete experimental setup for water transport including the gate's activation mechanism, temperature and pressure systems for a) 100% RH and b) 10 – 50 % RH.

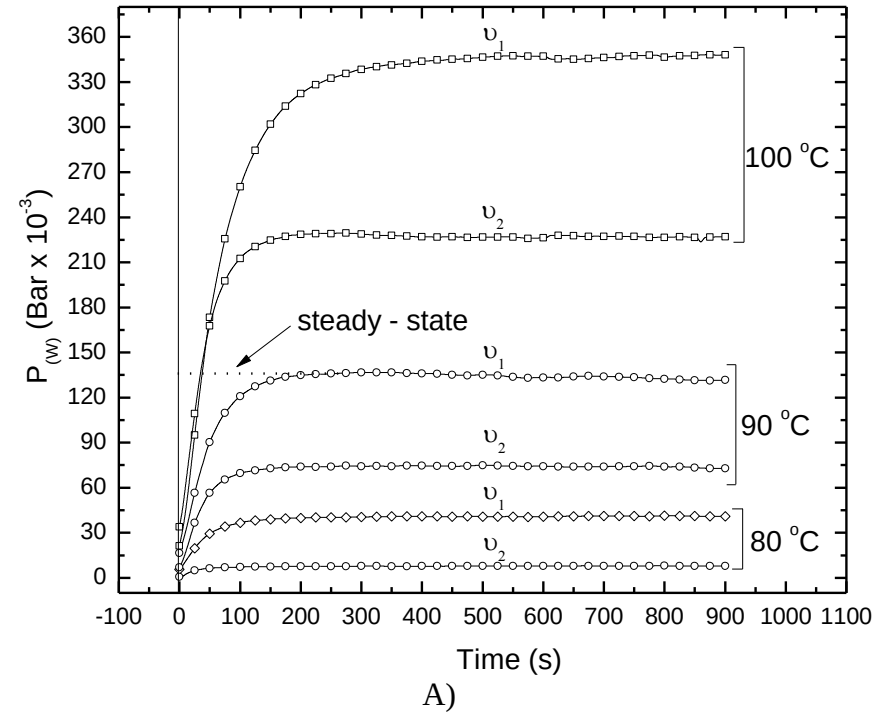

A)

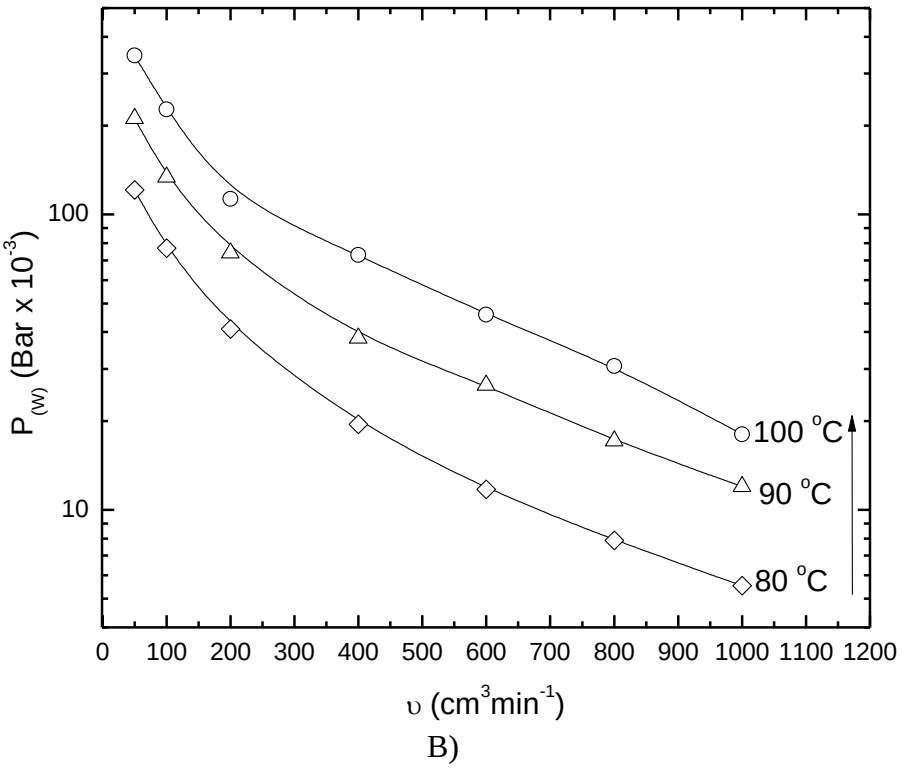

B)

Figure 2. a) Water vapor pressure signal vs time at different helium flow rates and temperatures and b) Water vapor pressure versus the helium flow rate, for the SiO_2-based membrane.

Before to start with the water flux experiments, a low helium flow (50 cm^3 min^{-1}) was introduced into the dry chamber in order to reach a steady state and then the pneumatic gate was open, exposing the membrane with the wet environment, and establishing a concentration gradient to drive

water across to the other side. Figure 2 (a) shows the experimental data obtained with the Vaisala® HMT 330 sensor, when the vapor pressure reached to steady – state, the average of the experimental data was taken obtaining the pressure value form the corresponding helium flow rate (υ). Then the pressure values were plotted as a function of the corresponding (υ). Figure 2b shows several data sets on vapor pressure under different temperatures, each point on the graph is an individual experiment obtained from Figure 2a.

The pressure data were obtained using the dew point temperature by the following equations (1 and 2) provided by the sensor's Vaisala [35]:

$$\Theta = T - \sum_{i=0}^{3} C_i T^i \quad (1)$$

$$\ln P_W = \sum_{i=-1}^{3} b_i \Theta^i + b_4 \ln \Theta \quad (2)$$

Where T is the dew point temperature (K), C_i and b_i are empirical coefficients [35] and P_w is the water pressure on the dry chamber. Finally with the data of vapor pressure, the water flux (J) was calculated, considering an ideal gas behavior and no water accumulation; the water flux (J) is defined as follow:

$$J_{VDP} = \frac{M_{VP} * \upsilon}{A} \quad (4)$$

Where M_{VP} is defined by the ideal gases equation (mol cm-3); ν is the helium flow rate (cm^3s^{-1}); and A, the membrane area (cm^2).

2.5 Fuel Cell Evaluation

The electrodes were made by the Ion Power Inc via spray, with a platinum loading of 0.3 mg Pt/C 30% E – Tek on the composite membranes. A carbon cloth with Teflon was used as gas diffusion layers. The performance test was carried in a single 5 cm^2 (Electrochem) connected to a Electrochem Compucell fuel cell test system. The Evaluation temperature was of 100 and 120 °C. The reaction gases were fed using a gases stoichiometry of 1.5 and 2 for H_2 and O_2 respectively, with a back pressure of 30 psi.

3. RESULTS

3.1 Physicochemical Characterization

The inorganic materials (SiO_2 and SBA–15) were subjected to X–ray diffraction (Figure 3). The diffraction patterns of the SiO_2 powder (Figure 3a) presented a maximum peak located at 24°

corresponding to the amorphous silica, these results confirm the existence of the silica powders. The SBA – 15 powder presented the same peak at 24° (Figure 3b). At small angles (Figure 3c) the SBA – 15 presented three peaks at 1, 1.5 y 2°, this signals are attributed to (1 1 0), (1 1 0) and (2 0 0) related with which are characteristic of a two-dimensional hexagonal phase of the SBA – 15. On previous work [36] reported a surface area of 1039 m^2 g^{-1} and 932 m^2 g^{-1} for SiO2 and SBA – 15 respectively, The water uptake, ion exchange capability and proton conductivity of composite membranes using SiO_2 and SBA – 15 were reported on previous work [37].

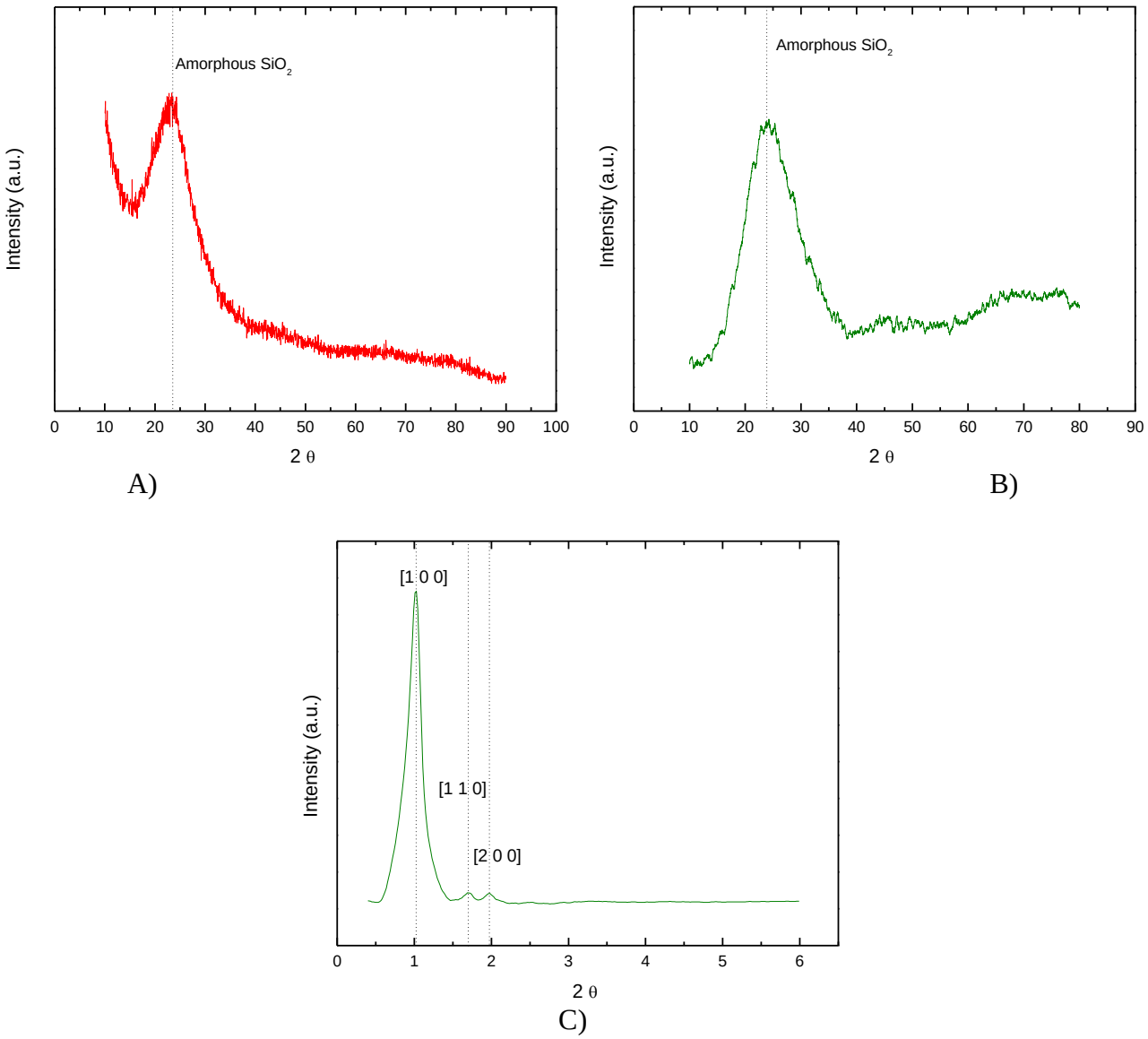

Figure 3. X-ray diffraction patterns of a) SiO_2, b) SBA – 15 powders and c) SBA – 15 at small angles.

Figure 4 shows the EDXS spectra of the SiO2 (a) and SBA – 15 (b) membranes. The spectra allowed identify the signals of Si on the membrane's surface and also the signals for C, F and S, characteristics of the Nafion Membrane. The morphology and EDXS mapping images are shown in

Figure 5. EDXS dot mapping was carried on each membrane for fluorine (F) (Figure 5a – II and 5b – II) and Silicon (Si) (Figure 5a – III and 5b – III).

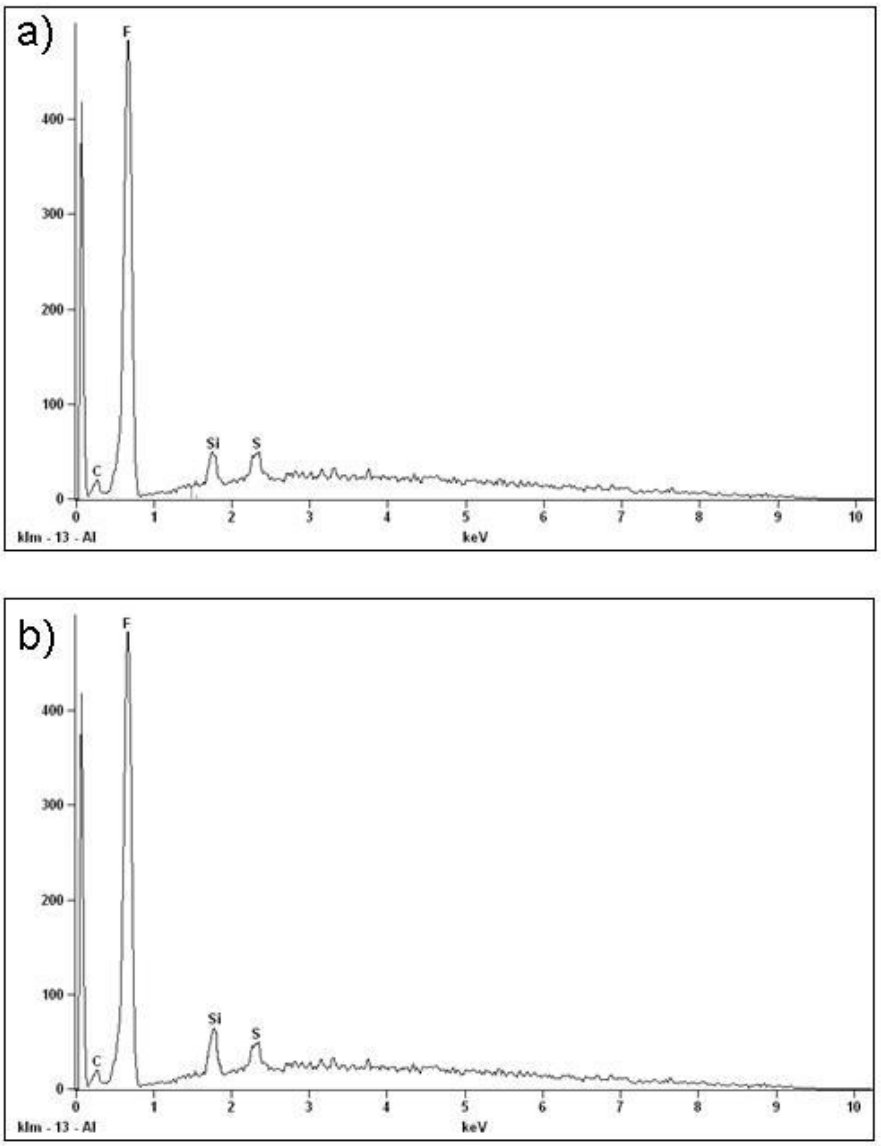

Figure 4. SEM images with a elemental mapping of (II) Fluoride and (III) Silicon for a) SiO_2 and b) SBA – 15 at 1500X.

As predictable, F is detected in all the membranes and it is corresponding to the Nafion structure. Si dispersion on the SiO_2 membrane (Figure 5a – III), indicates the formation of some agglomerations of SiO_2 on the membrane's surface. Si presence on SBA – 15 membrane (Figure 5b – III), the inorganic filler is homogeneous, with the formation of a minimal agglomeration of the material on the membrane.

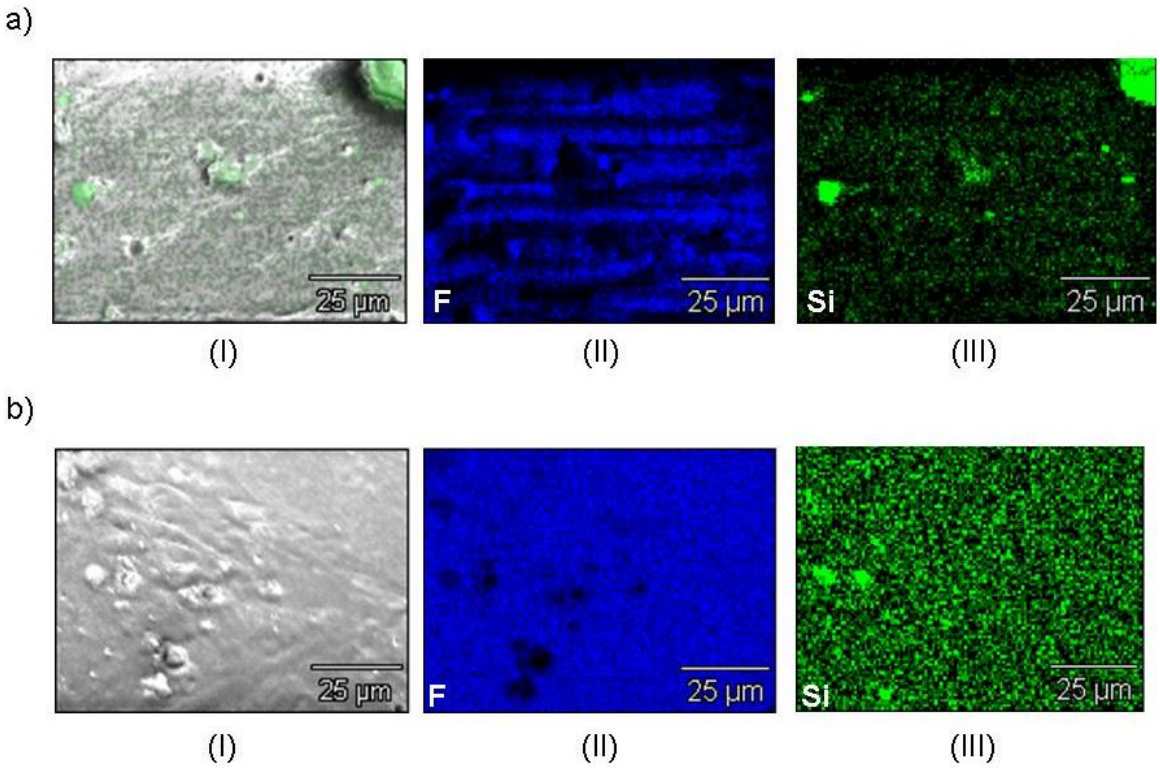

Figure 5. EDXS analysis of a) SiO_2 membrane and b) SBA – 15 membranes.

3.2. Water Transport Experiments

Complete water transport experiments are presented in Figures 6, 7 and 8.

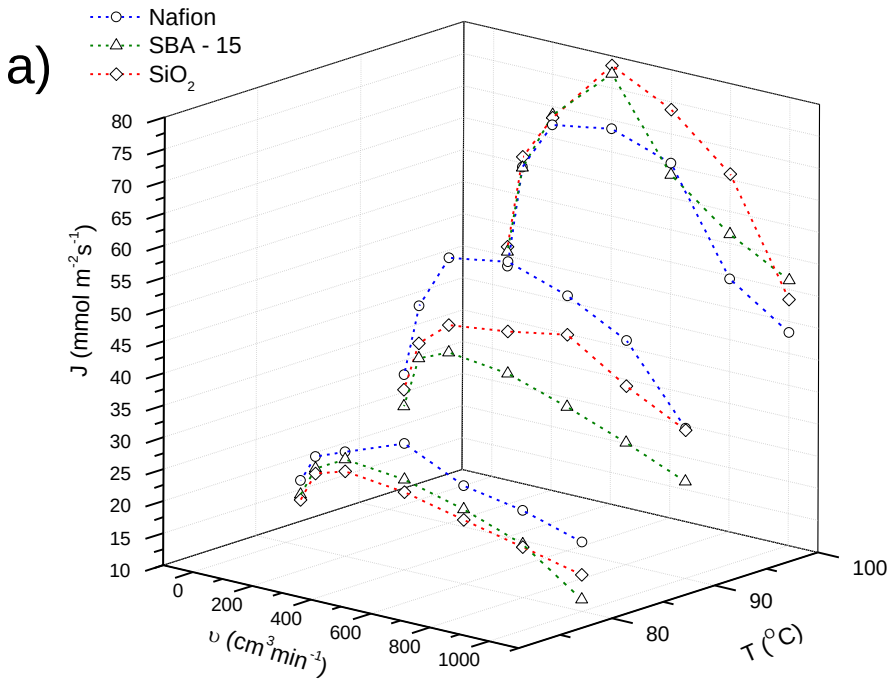

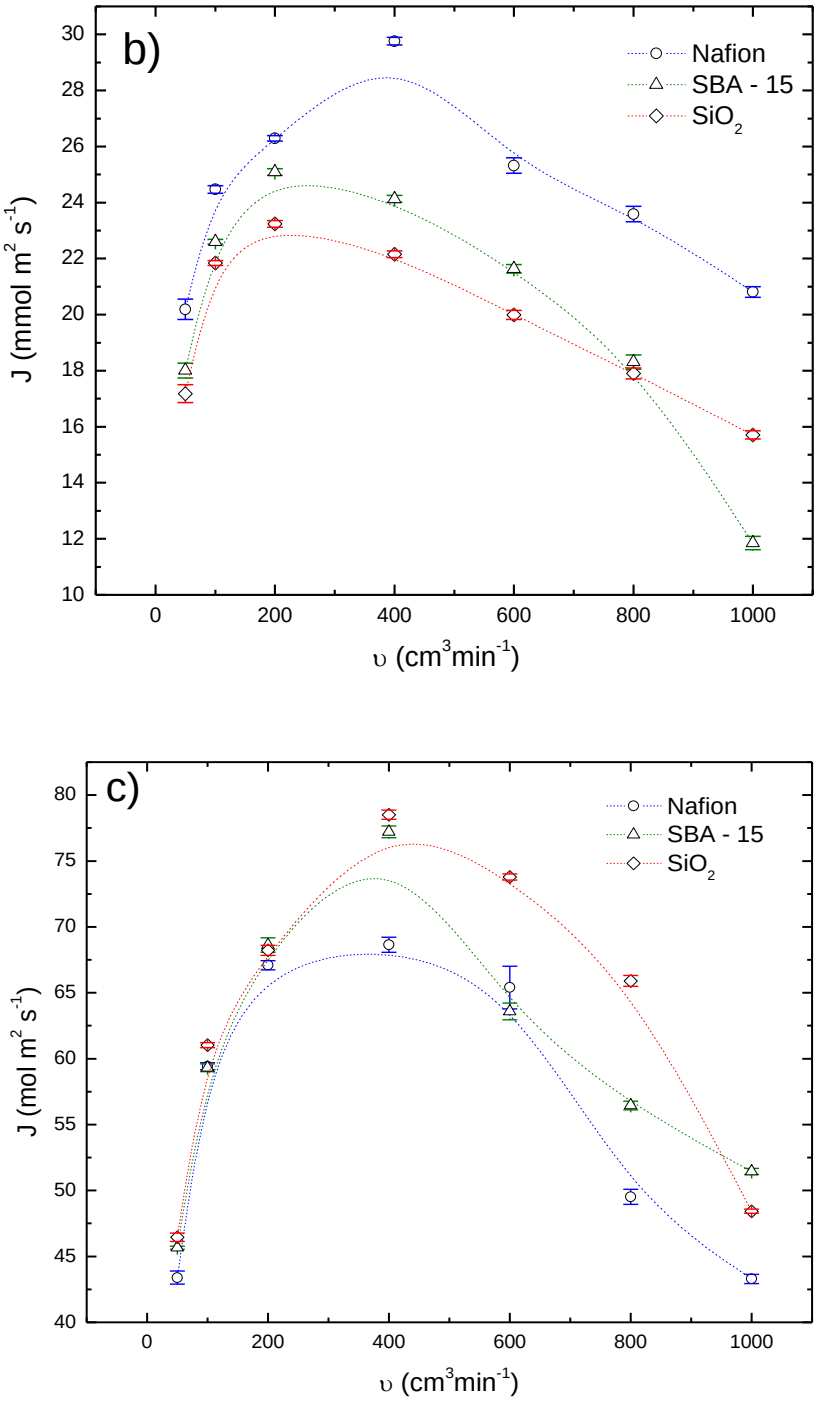

Figure 6. Steady – state water flux at 100 % RH at b) 80 and c) 100 °C.

Flux data showed an acceptable reproducibility with a maximum standard deviation of $5 \cdot 10^{-4}$ and a maximum standard error of $\pm$ $7 \cdot 10^{-4}$ mol m^{-2} s^{-1}. Within the experimental range of carrier-gas flow rates, the measured water flux increases, reaching a maximum, and later on decreases. This behavior has been previously observed [38, 39], suggesting that under these conditions, the water content is low in the region closer to the membrane's dry side (due to effect of the gas flow rate), and results in reduced pores sizes which could generate a hydrophobic surface [34]. Additionally,

Majsztrik et al. suggest that at high flow rates the surface of the membrane is dehydrated completely forming an impermeable skin which reduces or prevents the water transport [38, 39].

The main processes involved in the water transport (gas phase) through the membranes have at least five processes, i) interfacial transport across the membrane/water vapor interface, ii) diffusion into the membrane, iii) swelling of the membrane and accommodate the water in the sulfonic groups, iv) diffusion through the membrane and v) interfacial transport with the carrying gas [38].

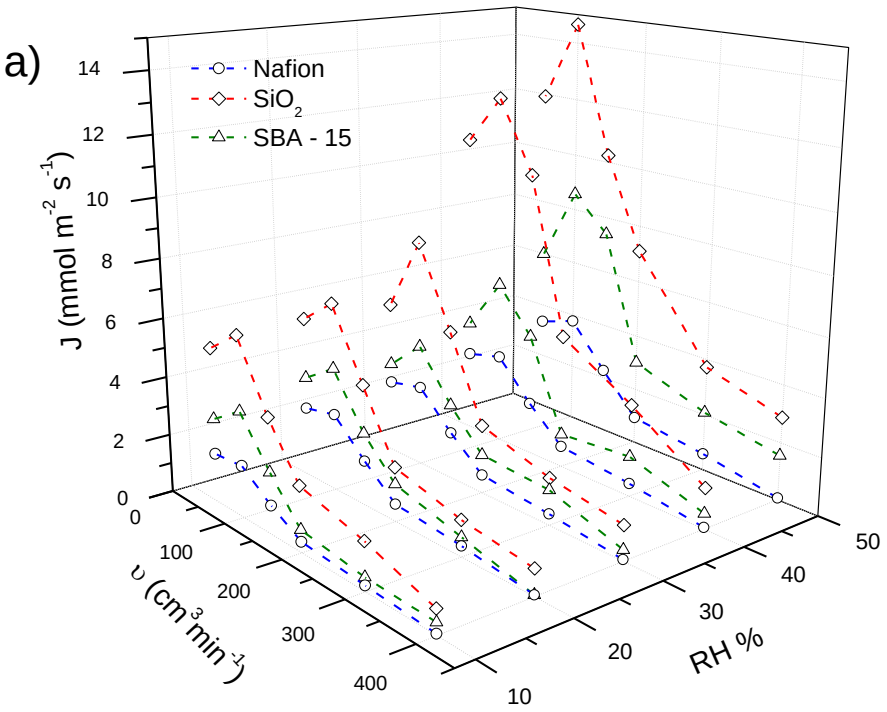

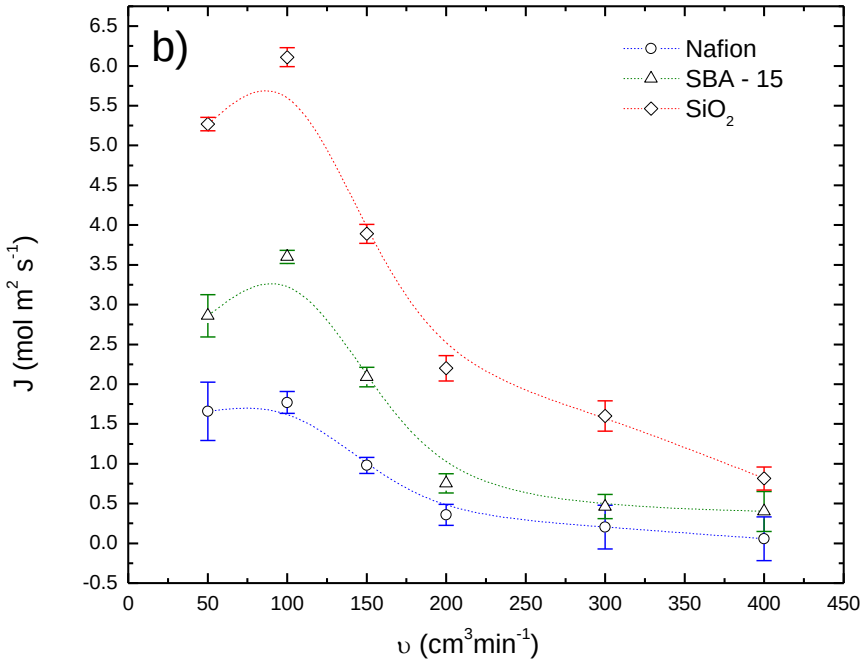

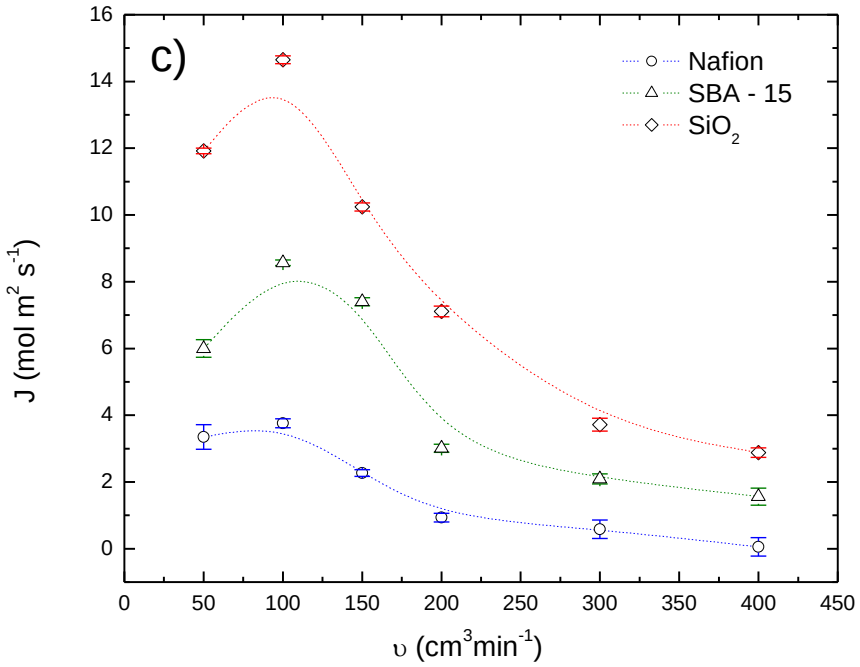

Figure 7. Steady – state water flux at 80 °C and b)10 and c) 50% RH.

Figure 6 a shows the measured water fluxes through the composite membranes at three different temperatures, the water fluxes increased with the temperature. The steady state water flux was plotted versus the helium flow rates (υ) at 80, 90 and 100 °C. At 80 ^{o}C (Figure 6 b), Nafion membrane has the larger water fluxes in the whole range of υ, with a maximum water flux around 29.7 mmol m^{-2} s^{-1} at 400 cm^3 min^{-1}. Composite membranes have the same trend that Nafion membrane with a maximum water flux at 200 cm^3 min^{-1}.

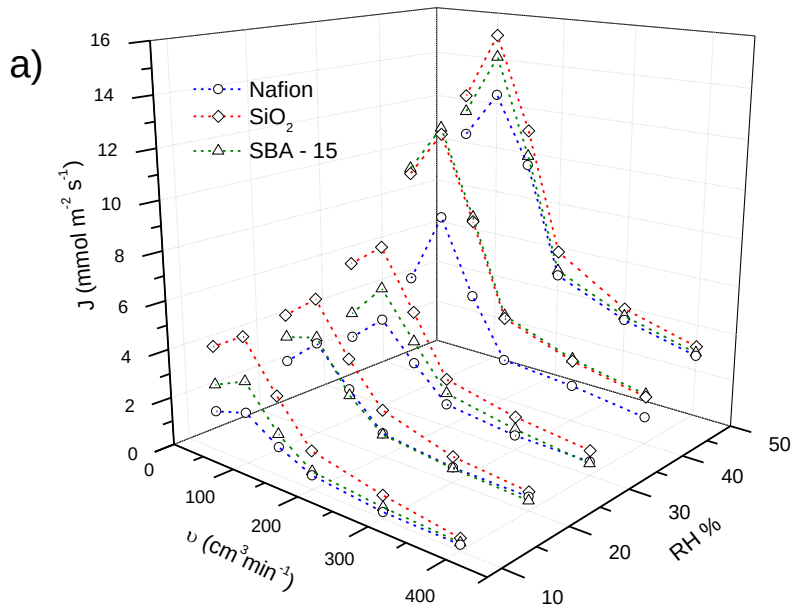

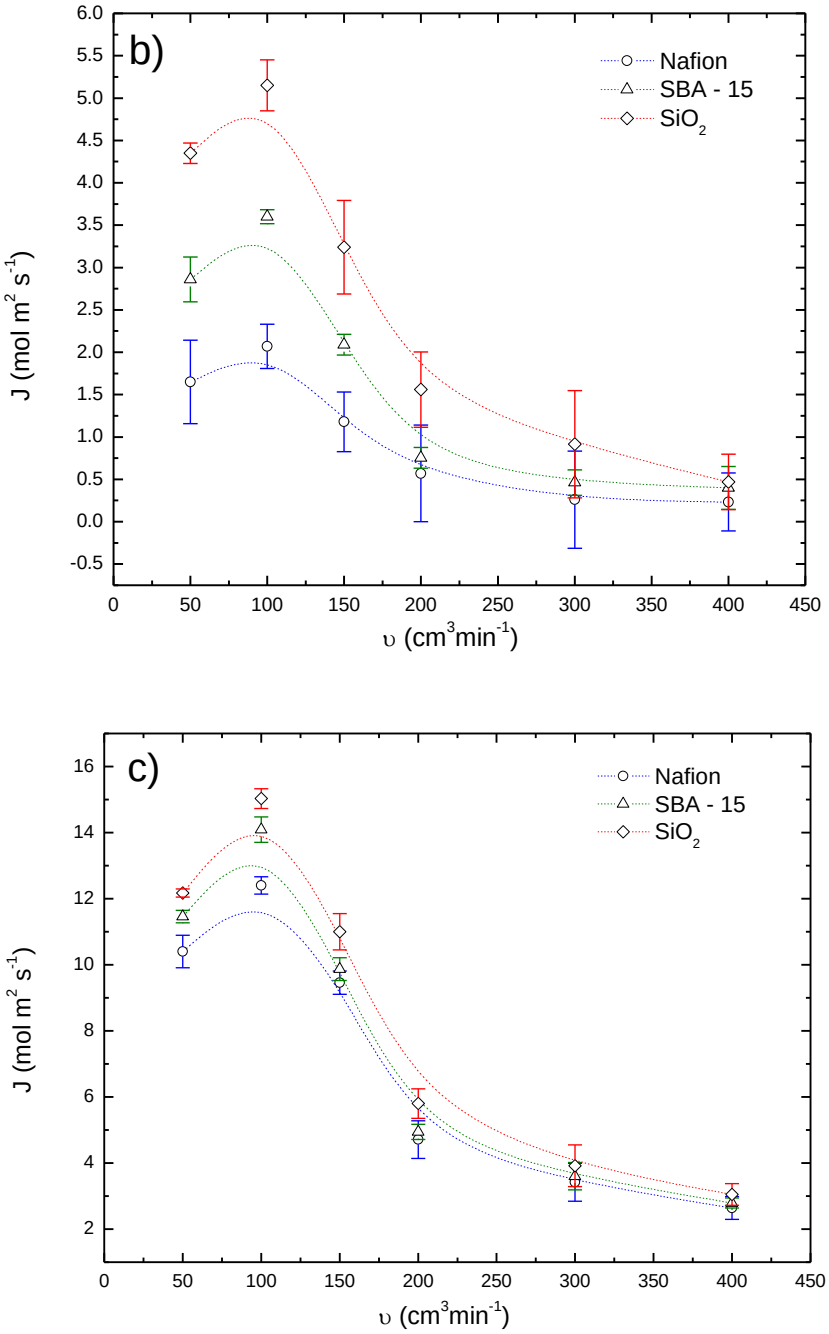

Figure 8. Steady – state water flux at 100 °C and b)10 and c) 50% RH.

SBA-15 composite membrane had the maximum water flux than the SiO_2 based membrane at low υ, however when the υ is 800 cm^3 min^{-1} or higher, the water flux on the SBA-15 membrane decreases dramatically. When the environment temperature increases to 90 ^oC, water flux on the membranes maintains the same tendency. In this case, Nafion membrane presents the maximum water flux in the whole range of υ. Composite membrane of SiO_2-based membrane increases the water flux compared with SBA-15 composite membrane.

In both cases Nafion membrane showed larger water flux than the composite membranes, this can suggest that Nafion membrane has an optimal environment to work ($\sigma \geq 10^{-2}$ Scm^{-1} and fully hydrated) [11]. At 100 ºC (Figure 6 c), composite membranes showed an increment in the water flux compared with the commercial membrane. SiO_2 membrane showed a maximum water flux (77 mmol m^{-2} s^{-1}) at 400 cm^3 min^{-1}. This value is larger than the other membranes. At high υ (1000 cm^3 min^{-1}), SiO_2 membrane suffers a decrement compared with the SBA-15 composite membrane.

Figure 7 and 8, show the results of experiments carried out at different RH values on the wet chamber; the υ was lower than that used in the experiments with 100% RH. The principal reason is due to in the wet chamber exists lower water content compared with at 100% RH and at high flow rates (above 400 cm^3 min^{-1}) on the dry chamber a hydrophobic layer is generated impeding the travel of the water through the membrane [38, 39].

Figure 7 showed the results at 80 ^oC. In all the relative humidity range, the composite membranes showed the larger water flux in the whole range of RH than the commercial membrane. SiO_2-based composite membrane showed the maximum water flux at 100 cm^3 min^{-1}, followed by SBA–15 composite membrane. At temperatures around 100 °C (Figure 8), the composite membranes had the same behavior than at 80 °C. The only difference is at RH of 40% (Figure 8), SBA–15 based membrane and SiO_2 composite membrane, have a similar water flux and when the RH increases to 50% (Figure 8 c). The difference between membranes is negligible, compared with the behavior at 80 °C. In the both cases, at different RH (80 °C and 100 °C), Nafion membrane exhibits a lower water flux compared with SiO_2-based composite membranes due to it is outside of its optimal operation conditions.

Water transport through Nafion membrane at 80 °C (Figure 9 a), is attributed ti the sulfonic acid groups and the hydrogen bonds interactions in the channel. The water molecules traveled via hopping mechanism inside the Nafion, at high humidity, water content is high ($\lambda \approx 14$), the connections between the channels are strong and high water flux data are obtained; however when the temperature of the system increases at 100 °C (Figure 9 b), the water content decreases ($\lambda < 14$) into the Nafion matrix and the connection between channels are weak. Introducing inorganic filler (Figure 9 c) with a temperature of 80 °C, the water transport is interrupted by the nanoparticles and it is reflected in low water flux data; but at temperatures of 100 °C (Figure 9b), the water flux increase because the inorganic filler entrapped water molecules into the Nafion and maintained the hydration of the membrane and the water transport is via hopping mechanism. Same behavior is observed at low relative humidity conditions (Figure 9 c).

The high water flux in the composite membranes, at high temperatures and low RH conditions is related with the interactions of the inorganic filler and the water molecules into the Nafion matrix. Water transport through a commercial membrane (Nafion) occurs as a function of the water content inside of the membrane. In regions with a low water concentration, the water is transported via diffusion through a structure of low porosity (low water content $\lambda < 14$) [34]. However, with the incorporation of inorganic fillers, the porosity increases improving the water content into the Nafion matrix ($\lambda \approx 14$), according to Aricò and coworkers [33], SiO_2 forms Si–OH interactions. OH groups facilities the water coordination acting as a water molecules trapping and vehicle molecule for proton migration. The water retained into the Nafion matrix helps to the diffusion of the water increasing the

water content into the membrane. The differences between SiO_2 and SBA– 15 water flux are mainly attributable to the hygroscopic characteristics and large surface area of fillers.

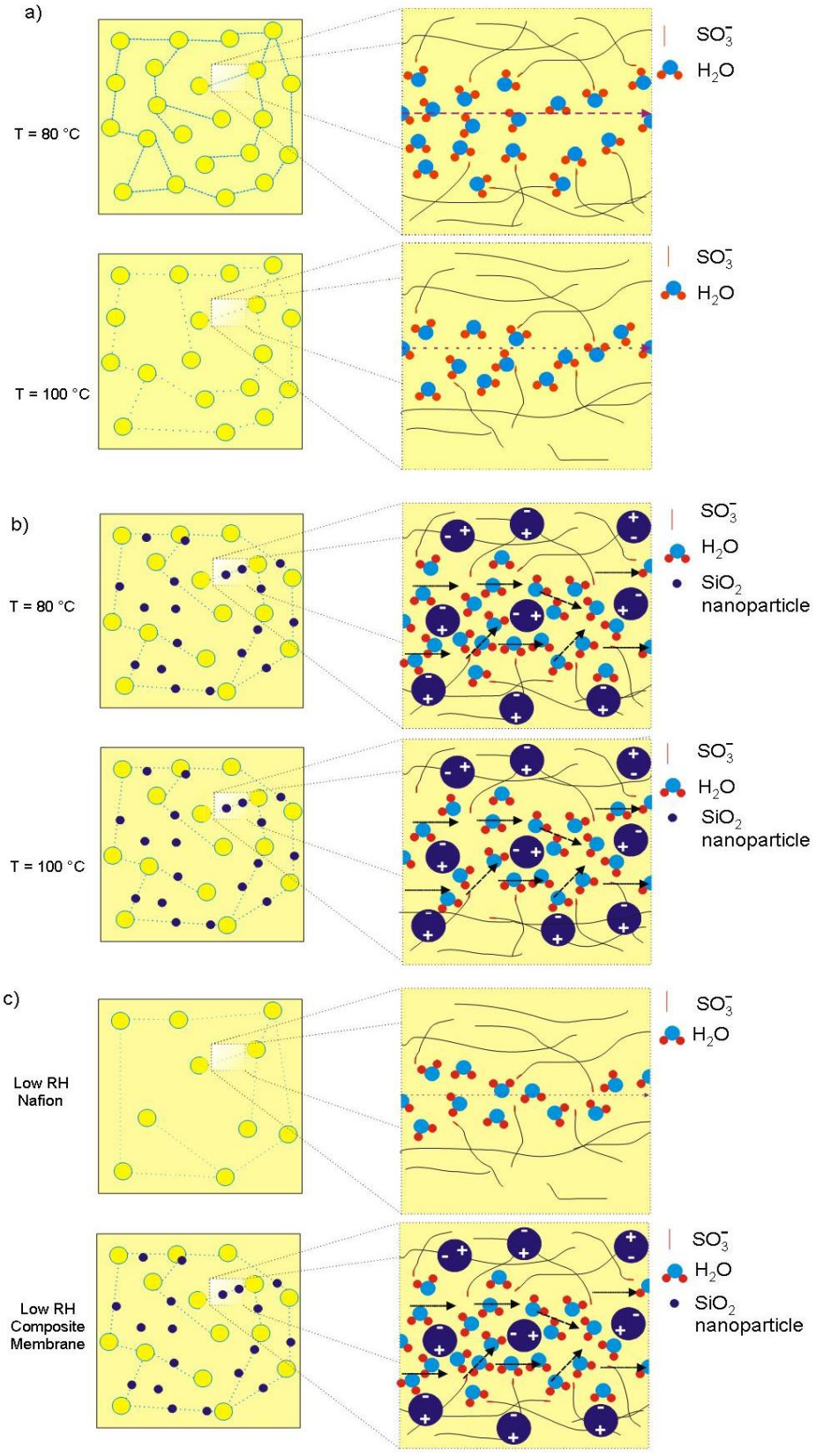

Figure 9. Proposed mechanism of water transport through: a) Nafion and b) Composite membranes.

BET results showed that the inorganic fillers based on SiO_2 offer high surface area: 1039 and 932 $m^2 g^{-1}$ for SiO_2 and SBA-15 respectively.

3.3 Fuel Cell Performance

On the fuel cell test (Figure 10), the composite membrane exhibited better performance than the commercial Nafion Membrane at low relative humidity and high temperature (100 and 120 °C).

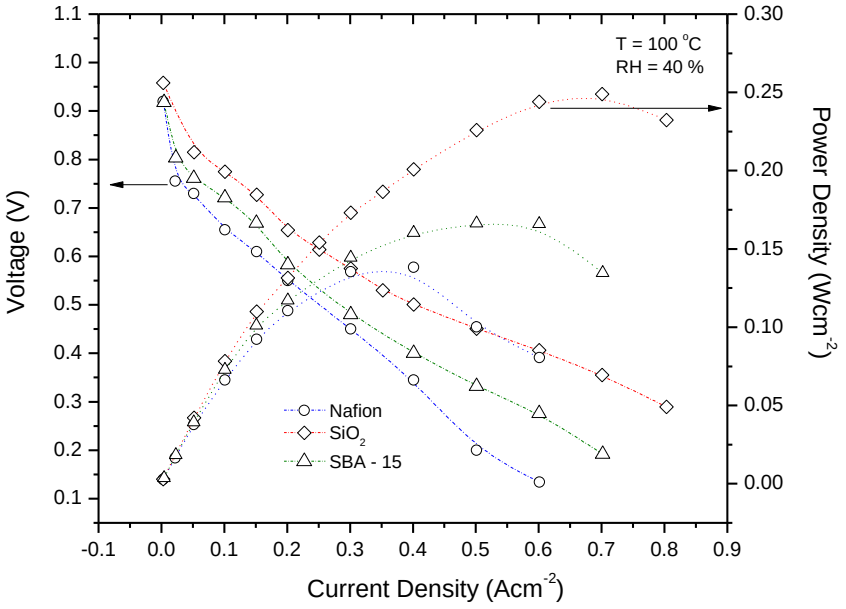

Figure 10. Polarization Curves of the composite membranes at a) 100 and b) 120 °C and 40 % of relative humidity.

In both temperatures the SiO_2 membrane showed better performance (0.25 and 0.14 Wcm^{-2} respectively) than the commercial Nafion membrane (around 0.13 Wcm^{-2}). This improvement in the composite membranes is due to the high water flux at high temperatures and low relative humidity, and also, the inorganic filler caused prevented temperature structural changes in the membrane, and maintained the membrane hydration [40].

The experimental results demonstrate that composite membranes based on SiO_2 improve the water flux at temperatures around 100 °C and low relative humidity than commercial Nafion membrane. The Fuel cell test showed that the composite membranes based in inorganic fillers as SiO_2 or SBA–15 as a promising alternative for elevated high temperature and low relative humidity PEMFC's applications.

4. CONCLUSIONS

Proton – exchange composite membranes were prepared from inorganic fillers with high superficial area, and characterized in terms of water flux at high temperature under simulated fuel cell conditions without the incorporation of a charge transfer and under extreme real operation conditions (100 and 120°C and 40% of relative humidity). Experimental results showed a larger water flux in composite membranes at high temperature (100 ºC) and low RH. The incorporation of inorganic fillers on the Nafion matrix increases the water flux due to the interactions dipole – dipole between the water and the composite nanoparticle maintaining the membrane hydration. SiO_2-based membranes have the maximum water transport compared with SBA–15 composite membrane, which could be attributed to higher superficial area in the case of SiO_2

ACKNOWLEDGMENTS

The authors want to thank Dr. Genoveva Hernández Padrón and M. Sc. Carmen L. Peza Ledesma from CFATA-UNAM, who carried out the FT – IR and Micro – Raman experiments. C. Guzmán, A. Alvarez and O.E. Herrera are grateful to Council for Science and Technology CONACYT for graduate fellowship. L.G. Arriaga and C. Guzmán gratefully acknowledge financial support from CONACYT through grant Fomix-Zacatecas 81728 and SEP-Conacyt 2009-133310.

References

1. P. Costamagna, C. Yang, A. B. Bocarsly and S. Srinivasan, *Electrochimica Acta*, 47 (2002) 1023-1033.
2. R. K. A. M. Mallant, *Journal of Power Sources*, 118 (2003) 424-429.
3. J. Zhang, Z. Xie, J. Zhang, Y. Tang, C. Song, T. Navessin, Z. Shi, D. Stong, H. Wang, D. P. Wikilnson, Z. Liu and S. Holdcroft, *Journal of Power Sources*, 160 (2006) 872 - 891.
4. S. Mukerjee and S. Srinivasan, *Journal of Electroanalytical Chemistry*, 357 (1993) 201-224.
5. K. T. Adjemian, S. J. Lee, S. Srinivasan, J. Benziger and A. B. Bocarsly, *Journal of The Electrochemical Society*, 149 (2002) A256-A261.
6. S. K. Das, A. Reis and K. J. Berry, *Journal of Power Sources*, 193 (2009) 691-698.

7. H. P. Dhar, L. G. Christner, A. K. Kush and H. C. Maru, *Journal of The Electrochemical Society*, 133 (1986) 1574-1582.
8. L. Qingfeng, H. Ronghuan, G. Ji-An, J. Jens Oluf and J. B. Niels, *Journal of The Electrochemical Society*, 150 (2003) A1599-A1605.
9. Y. Shao, G. Yin, Z. Wang and Y. Gao, *Journal of Power Sources*, 167 (2007) 235-242.
10. C. Song, Y. Tang, J. L. Zhang, J. Zhang, H. Wang, J. Shen, S. McDermid, J. Li and P. Kozak, *Electrochimica Acta*, 52 (2007) 2552-2561.
11. G. Alberti, M. Casciola, L. Massinelli and B. Bauer, *Journal of Membrane Science*, 185 (2001) 73-81.
12. C. M. Bautista-Rodríguez, A. Rosas-Paleta, J. A. Rivera-Márquez and O. Solorza-Feria, *International Journal of Electrochemical Science*, 4 (2009) 43 - 59.
13. C. M. Bautista-Rodríguez, A. Rosas-Paleta, J. A. Rivera-Márquez and O. Solorza-Feria, *International Journal of Electrochemical Science*, 4 (2009) 60 - 76.
14. T. A. Zawodzinski, D. Charles, R. Susan, J. S. Ruth, T. S. Van, E. S. Thomas and G. Shimshon, *Journal of The Electrochemical Society*, 140 (1993) 1041-1047.
15. N. H. Jalani, K. Dunn and R. Datta, *Electrochimica Acta*, 51 (2005) 553-560.
16. T. Jian-hua, G. Peng-fei, Z. Zhi-yuan, L. Wen-hui and S. Zhong-qiang, *International Journal of Hydrogen Energy*, 33 (2008) 5686-5690.
17. A. Saccà, I. Gatto, A. Carbone, R. Pedicini and E. Passalacqua, *Journal of Power Sources*, 163 (2006) 47-51.
18. M. P. Rodgers, Z. Shi and S. Holdcroft, *Journal of Membrane Science*, 325 (2008) 346-356.
19. H. Li, Y. Tang, Z. Wang, Z. Shi, S. Wu, D. Song, J. Zhang, K. Fatih, J. Zhang, H. Wang, Z. Liu, R. Abouatallah and A. Mazza, *Journal of Power Sources*, 178 (2008) 103-117.
20. M. Watanabe, H. Uchida and M. Emori, *Journal of Physical Chemistry B*, 102 (1998) 3129-3137.
21. K. Flodström and V. Alfredsson, *Microporous and Mesoporous Materials*, 59 (2003) 167-176.
22. R. Huirache-Acuña, B. Pawelec, E. Rivera-Muñoz, R. Nava, J. Espino and J. L. G. Fierro, *Applied Catalysis B: Environmental*, 92 (2009) 168-184.
23. R. Nava, B. Pawelec, P. Castaño, M. C. Álvarez-Galván, C. V. Loricera and J. L. G. Fierro, *Applied Catalysis B: Environmental*, 92 (2009) 154-167.
24. D. H. Aguilar, L. C. Torres-González, L. M. Torres-Martínez, T. López and P. Quintana, *Ciencia UANL*, 6 (2003) No. 1.
25. J. González-Hernández, J. F. P. Robles and J. R. M. F. Ruiz, *Superficies y Vacío*, 11 (2000) 1 - 16.
26. S. Melada, M. Signoretto, S. A. Ardizzone and C. L. Bianchi, *Catalysis Letters*, 75 (2001) 199-204.
27. A. Morales-Acevedo and G. F. Pérez-Sánchez, *Superficies y Vacío*, 16 (2003) 16-18.
28. R. Pérez-Hernández, J. Arenas-Alatorre, D. Mendoza-Anaya, A. Gómez-Cortés and G. Díaz, *Revista Mexicana de Física* 50 (2004) 80-84.
29. M. L. Rojas -Cervantes, R. M. Martin -Aranda, A. J. Lopez -Peinado and J. D. D. Lopez -Gonzalez, *Journal of Materials Science*, 29 (1994) 3743-3748.
30. V. Santos, M. Zeni, C. P. Bergmann and J. M. Hohemberger, *Rev.Adv.Mater.Sci*, 17 (2008) 62-70.
31. A. S. Arico, P. Creti, P. L. Antonucci and V. Antonucci, *Electrochemical and Solid-State Letters*, 1 (1998) 66-68.
32. V. Antonucci, A. Di Blasi, V. Baglio, R. Ornelas, F. Matteucci, J. Ledesma-Garcia, L. G. Arriaga and A. S. Aricò, *Electrochimica Acta*, 53 (2008) 7350-7356.
33. A. S. Arico, V. Baglio, A. Di Blasi, P. Creti, P. L. Antonucci and V. Antonucci, *Solid State Ionics*, 161 (2003) 251-265.
34. T. Romero and W. Mérida, *Journal of Membrane Science*, 338 (2009) 135-144.
35. *Vaisala Report M210566EN – C*, (2005)
36. A. Alvarez, C. Guzmán, C. P.-. Ledesma, L. A. Godínez, R. Nava, S. M. D.-. Torres, J. L.-. Farcía and L. G. Arriaga, *Journal New Materials for Electrochemical Systems*, 14 (2011) (*In press form*).

37. A. Alvarez, C.Guzmán, A.Carbone, A.Saccà, I.Gatto, R.Pedicini, E.Passalacqua, R.Nava, R. Ornelas, J.Ledesma-García and L.G.Arriaga, *Journal Power Sources*, A.Alvarez,etal.,J.PowerSources(2011),doi:10.1016/j.jpowsour.2011.02.072 (2011)
38. P. W. Majsztrik, M. B. Satterfield, A. B. Bocarsly and J. B. Benziger, *Journal of Membrane Science*, 301 (2007) 93-106.
39. P. W. Majsztrik, M. B. Satterfield, A. B. Bocarsly and J. B. Benziger, *ECS Transactions*, 11 (2007) 609-621.
40. C. Guzmán, A. Alvarez, O. E. Herrera, L. A. Godínez, W. Mérida, J. L.-. García and L. G. Arriaga, *Journal New Materials for Electrochemical Systems*, 14 (2011) XXX(In press Form).